# TECHNICAL REPORT

OMMATIDIA
A NEW LOOK AT LIDAR

COMET INGENIERÍA

**PROJECT**

**In-orbit surface metrology for large deployable reflectors**

**ESA Contract No: 4000130881/20/NL/RA**

**TITLE**

## Executive Summary Report

| | | | |
|---|---|---|---|
| **REFERENCE** | **1dPr8UIUxQC-K4aOHJbReMA35tyw-T5YD** | **ISSUE** | **2** |

**CUSTOMER**

**ESA-ESTEC (European Space Agency)**

| **Focal point:** |
|---|
| Shumit Das |
| |
| |


**SUMMARY**

In the frame of the ESA Contract for in-orbit surface metrology for deployable reflector missions, this document presents the "executive summary report", that concisely summarizes the findings of the contract.




| **Authors:** | **Approved:** |
|---|---|
| **Ivan Bravo (Ommatidia)**<br>**Gregory Pandraud (Ommatidia)** | **Eduardo Margallo (Ommatidia)** |
| **Date:** 20-April-2023 | **Date:** 21-April-2023 |

| | | | |
|---|---|---|---|
| **Project:** | In-orbit surface metrology for large deployable reflectors | | |
| **Title:** | Executive Summary report | | |
| **Customer:** ESA-ESTEC | **Ref.:** 1dPr8UIUxQC-K4aOHJbReMA35tyw-T5YD | | **Issue:** 2 |

## RECORD OF REVISIONS

| Issue | Responsible | Modification | Affected pages | Date |
|---|---|---|---|---|
| 1 | Grégory Pandraud (GP) and Iván Bravo (IB) | Original issue | - | 13-05-2022 |
| 2 | Grégory Pandraud (GP) and Iván Bravo (IB) | CCN information | - | 21-04-2023 |
| | | | | |
| | | | | |
| | | | | |
| | | | | |
| | | | | |
| | | | | |
| | | | | |

## LIST OF DISTRIBUTION

| Name | Company/Department | Via | Date |
|---|---|---|---|
| Shumit Das | ESA | Email | 25-05-2022 |
| | | | |
| | | | |
| | | | |

## CONTENTS

## 1. INTRODUCTION

Recently, an increasing number of space missions are starting to make use of Large Deployable Reflectors (LDRs), especially in applications such as Earth observation (e.g., SAR, radiometers) and Telecom. In order to achieve a good performance of such as structures for the application in hand, a precise knowledge of the reflector surface and pointing accuracy in-orbit is essential. For this reason, there is a growing demand for metrology technologies that can provide an accurate characterization of the LDR, while being capable to work under the extreme environment of space and taking into account the severe resource limitations of working in space.

To date there is no commercial system in the market that is completely suitable for calibration of LDRs in-orbit due to different reasons. Typical ground metrology systems such as laser trackers [1,2], laser scanners [3] and photogrammetric system[2,4,5] offer high accuracy at long distance needed to characterise LDRs working in the Ka-Band frequency range. However, it would be very impractical to bring such systems to space as these have high volume, mechanical scanners that will suffer during launching, high power consumption and need a human technical operator. On the other hand, other ground metrology technologies such as standard LiDARs (Time-of-flight)[6] cannot offer the accuracy required for LDRs, being always above a few cm. Apart from these metrology technologies, techniques like structured-light projection (used to characterise heliostats in concentrated solar power field)[5], iGPS[6] and even Fiber Bragg Gratings (FBGs)[7] have been considered. However, none of these technologies are suitable for space as they cannot be implemented such as a structure light projection. Regarding FBGs, this technology required an in-built FBG on the LDR, which could cause distortions in the normal operation of the LDR and it is considered a contact measurement. Furthermore, the accuracy is not as good as, for instance, laser trackers or photogrammetry.

Even if most of the technologies described above can be used for characterization of LDRs in-ground, however, there is a lack of solutions for in-orbit operation that can fully satisfy the required demands for in-orbit surface characterization of LDRs.

## 2. OMMATIDIA LIDAR TECHNOLOGY

LiDAR systems developed by Ommatidia LiDAR belong to the so-called frequency modulated continuous wave (FMCW) LiDARs. While time-of-flight (ToF) LiDARs measure distances based on the time that a pulse from the pulsed-laser takes to come back to the detector, FMCW LiDARs measure beat frequencies to obtain the distance information. For that, a continuous wave frequency modulated laser is needed, meaning that the instantaneous frequency of the laser varies with time. The range of frequencies (wavelengths), in which the laser can be modulated, is called frequency excursion. In brief, the operation of the LiDAR is the following: by illuminating the target with a frequency-modulated continuous wave (local oscillator), the reflected signal from the target is received having a delay with respect to the local oscillator. The reflected signal from the target is received by an array of waveguides, which have a field of view (FoV) that covers the entire scene. Then, both the local oscillator signal (reference arm) and the received signal (sample arm) are mixed in an interferometer and detected coherently with a sensor. Detection is shot noise limited, being an advantage over other systems as the system has single photon sensitivity. After transforming the mixed signal from the time domain to the frequency domain, the resulting beat frequency is retrieved, which is related to the distance information.

For the illumination of the LDR we chose a discrete illumination of the LDR (a fixed number of beams with known directions with a diffractive optics beam splitter) together with the use of film retroreflectors. Retroreflective targets that are often discarded for space missions can be added to the LDR (in this project in the form of adhesive film retroreflectors) or embedded into the LDR.

**Preliminary performance assessment**

Having decided on the illumination approach of the LDR using a diffractive optics beam splitter to divide the laser beam in different replicas (Fig. 1), the preliminary performance of the metrology breadboard was evaluated by means of an optical simulator developed for this purpose. The simulator works on the basic principle of Ommatidia LiDAR technology explained above.

Results from the simulations show that for a fixed laser output optical power of 1.25 W, RMS distance accuracy below 10 µm can be achieved with the metrology breadboard for a wide range of integration times (above 1s) and frequency excursions larger than 40 GHz. This is within the capabilities of current lasers and cameras previously used by Ommatidia LiDAR. Therefore, better distance accuracy can be obtained either by increasing the integration time (measurement time) or increasing the frequency sweep of the laser. Furthermore, an increase of laser power can also help in achieving the required accuracy, but at the cost of having a bigger laser, which could result in larger power consumption and higher volume. In any case, all these numbers were taken into account during the design and manufacturing phase in order to achieve the best performance, while keeping the system compact and resources to the minimum possible.

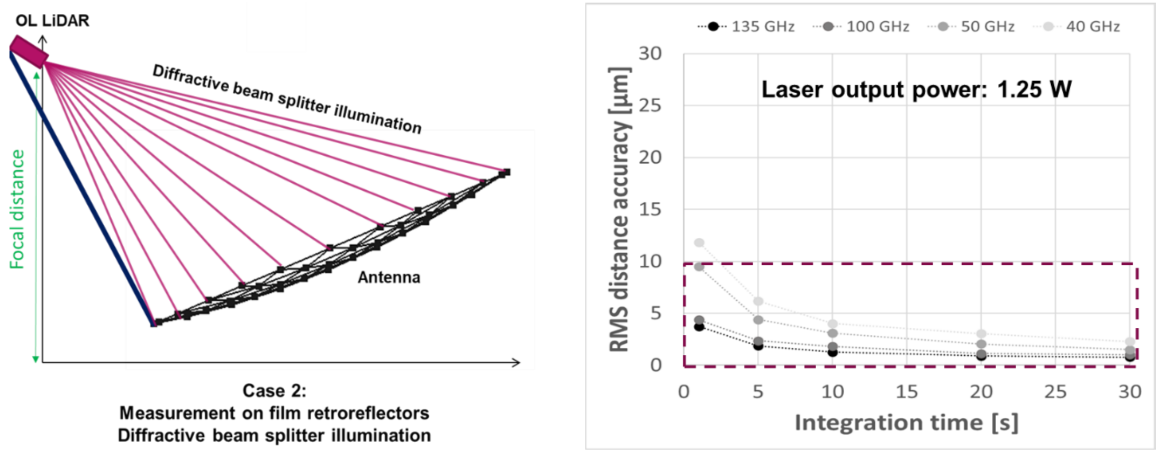


**Figure 1. Left: Schematic of the measurement setup of the metrology breadboard (discrete illumination of the LDR). Right: RMS distance accuracy as a function of integration time and frequency excursion of the laser for 1.25 W of total output optical power.**

In order to compare the results achieved with the proposed LiDAR with a known ground technique, photogrammetry was chosen, and it can reach accuracies down to 50 µm. As described later this first estimation has proven to be on the high side allowing a perfect result comparison.

## 3. Breadboard Design and Manufacture

The breadboard developed by Ommatidia LiDAR for the metrology breadboard is shown in Fig. 2. The main parts of the metrology breadboard are: 1) Illumination: this part consist of a high-power and low-noise continuous wave (CW) Distributed Feedback (DFB) diode laser and a fiber amplifier to increase the output optical power of the system up to 5 W. After that, the IR light is collimated and sent to a diffractive optical element (DOE) that splits the single beam from then laser into an array of 10x10 points with angular separation of 4.46 degrees. These 100 beams are the ones that are sent to the LDR and thus the points that will be measured from it. 2) Collection: this part of the system is a microscope objective (Fig. 3) to adapt the field of view (FoV) of the metrology breadboard in order to capture all the illuminated points. 3) Receiver (3D receiver sensor + photodetector array): the 3D receiver sensor shown in Fig. 4 is the core of Ommatidia LiDAR technology. When the IR light is reflected back from the 100 illuminated points, this passes through the microscope objective and then it is collected by the 3D receiver sensor by means of an array of grating couplers, shown in Fig. 4, that couples the light into the sensor. This allows to collect the light from the entire scene without the need of any mechanical scanner. The 3D receiver sensor is made on a silicon nitride platform. In order to increase the coupling efficiency of the light captured by the array of gratings of the 3D receiver sensor, this was thinned down to 150 μm and a microlens array (MLA) was placed on top of it, as shown in Fig. 4.

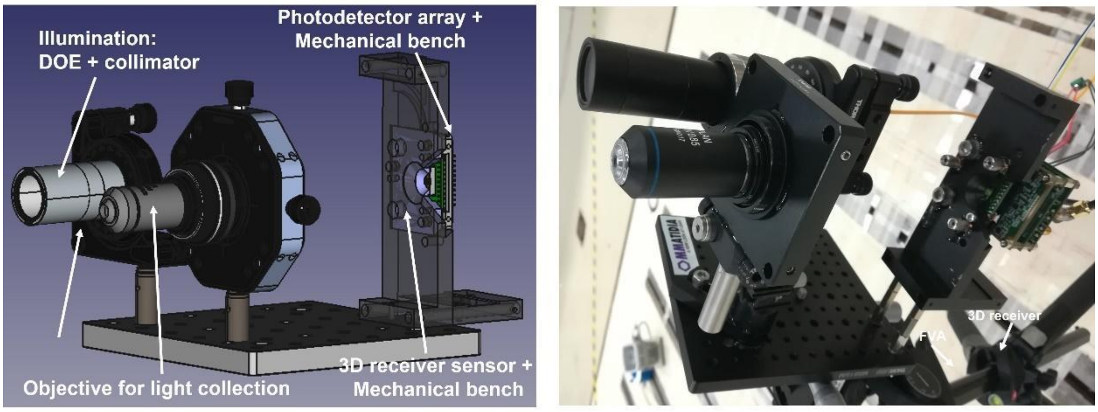


**Figure 2. Left: Design of the metrology breadboard with the main parts and components highlighted. Right: Implementation of the developed metrology breadboard.**

After the IR light is collected by the 3D receiver sensor, this is mixed with the reference signal from the laser source entering the 3D receiver sensor from the reference channel (Fig. 4) using a fiber V-groove array (FVA) attached to the chip. Eventually the mixed signal is guided to the detection (output) gratings, and collected by a photodetector array that converts the optical information into electrical signals. The postprocessing in a computer gives the distance information and a point cloud of the surface shape of the LDR can be generated.

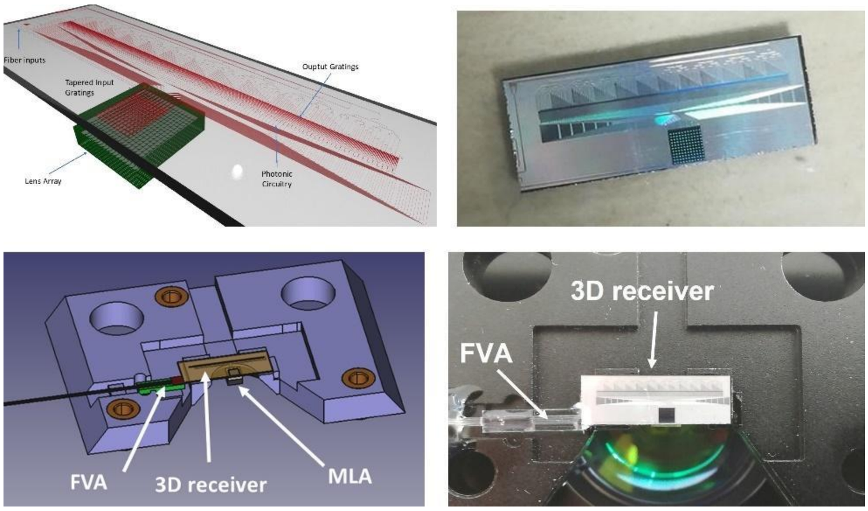


**Figure 4. 3D receiver sensor, core of Ommatidia LiDAR technology. Top: Design and implementation of the 3D receiver sensor (integrated photonic circuit) that collects light from the scene for optical mixing. Bottom: Packaging of the 3D receiver sensor, including mechanical bench, fiber V-groove array for reference signal and microlens array.**

## 4. Test Setup

The final setup of the LDR, is shown in Fig. 5. After the assembly of the LDR at Tekniker (Spain), coded retroreflector targets were installed on the reflector mesh for comparison between photogrammetry and Ommatidia's metrology breadboard. Two types of coded markers were used, shown in Figs. 5 and 6: 1) 100 coded targets (measurement points on the LDR) for which its position (x, y, z) will be determined and compared by both techniques; 2) additional 852 coded targets for best accuracy of photogrammetry. The position of the coded targets on the mesh is determined by the projection of a grid of 10x10 IR points given by the DOE of the metrology breadboard, when placed in the final measurement position.

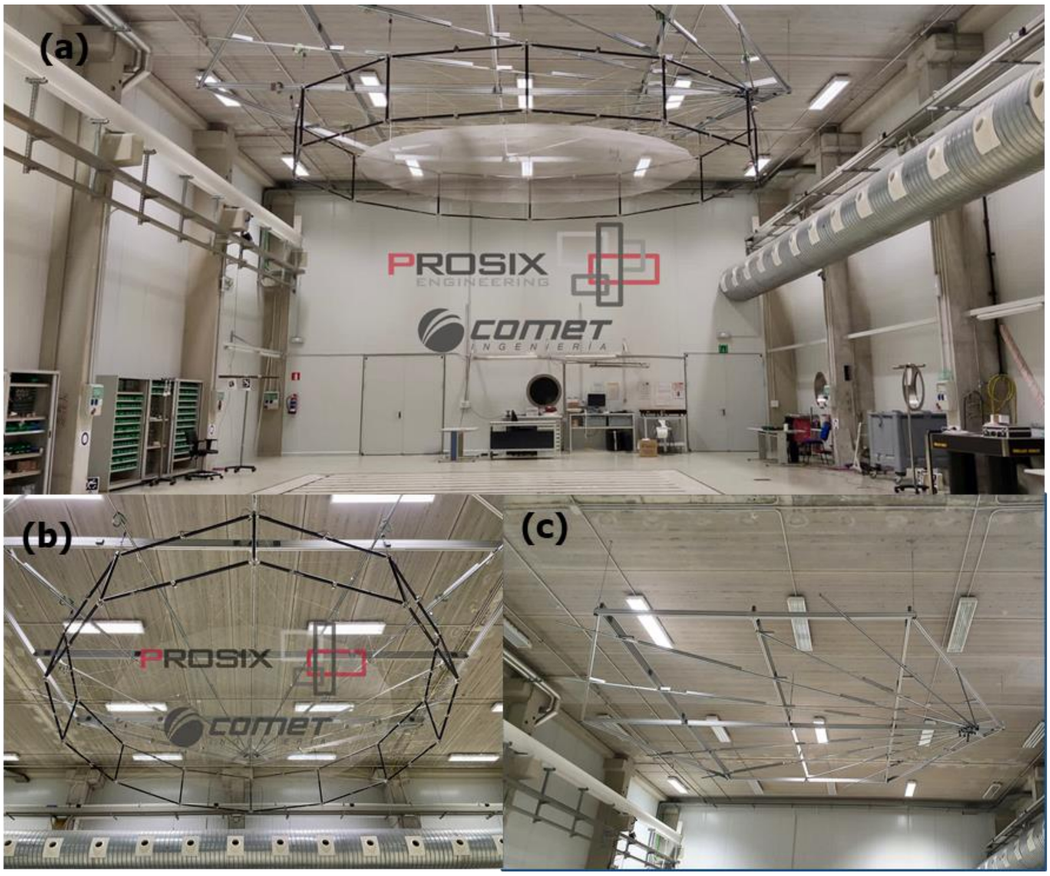


**Figure 5. LDR setup in the high-precision chamber at Tekniker.**

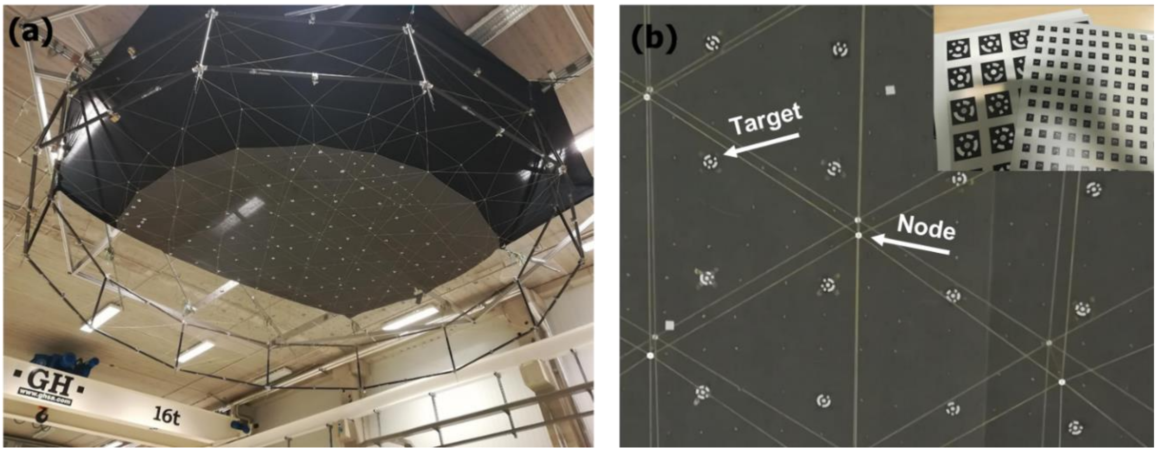


**Figure 6. Coded retroreflector targets on the reflector mesh. (a) Final LDR setup with coded targets. (b) Detail of the reflector mesh.**

## 5. Performance Evaluation of the Breadboard

During the test campaign, different configurations of the breadboard were investigated in order to achieve the best performance of the system, attempting to minimise the resources needed in space, mostly power supply for a fixed mechanical structure of the system. The configuration used during the final measurements is summarised in Table 1.

**Table 1. Configuration of the breadboard during the measurements.**

| Parameters | Value |
|---|---|
| **Total output optical power** | 3 W |
| **Output optical power per point** | 30 mW |
| **Power consumption of the system** | 38.4 W |
| **Integration time** | 1 s |
| **Frequency sweep of the laser** | 35 GHz |
| **Distance illumination (DOE) – LDR (central node)** | 4 m |
| **Field-of-view of the system** | 42 degrees |

With the metrology breadboard placed at 4 m (see table) from the LDR, a set of 300 measurements of 1 s were taken to determine the repeatability of the system for each of the points, which is used as a measure to evaluate the performance of the breadboard. Repeatability is calculated as the standard deviation of the measured frequency over the 300 measurements. Figure 7 shows a measurement of the mean intensity of each of the points measured normalised to the noise floor (Fig. 7a), given as a SNR value for 300 measurements. Moreover, the repeatability measure is shown in Fig 7b. Both results are given in the reference system of the 3D receiver in pixels. Figure 8 shows the point cloud generated by the breadboard (x, y, z components) that will be compared against the photogrammetric point cloud to evaluate the accuracy of the metrology breadboard.

The current version of the metrology breadboard is able to carry out measurements of 100 points on a LDR in 1 s, resulting in points having repeatability below 150 μm. However, we believe that solving the aberration issue and having a SNR of at least 30 dB in all the points will result in all the 100 points having a repeatability below 100 μm.

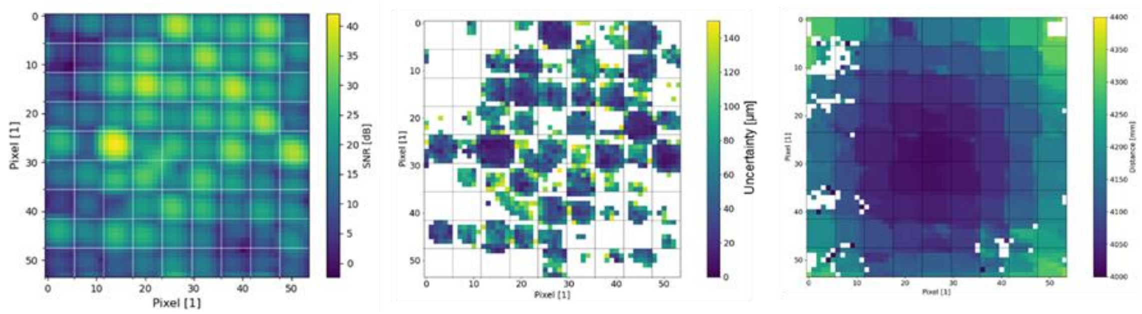


**Figure 7. Measured target points on the LDR mesh. (a) Signal-to-noise ratio (SNR) of each point, and (b) repeatability performance over 300 measurements. Points not shown in the repeatability graph (b) are above 100 μm.**

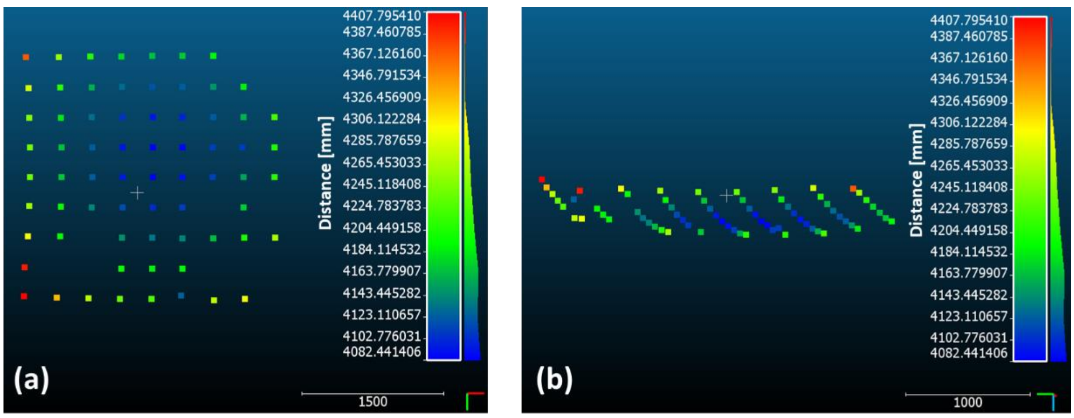


**Figure 8. Point cloud of the points measured on the LDR by the metrology breadboard. Distance is shown in mm.**

Finally, the point cloud generated by the metrology breadboard was compared with the one given by the ground-based baseline (photogrammetry). The registration of both point clouds is shown in Fig. 9, where the surface given by the photogrammetry point cloud and the best points (best SNR and repeatability) are used for the comparison. Figure 10 shows the accuracy of the points with better SNR (above 20 dB) with respect to the surface given by the photogrammetry point cloud. The rest of the points were discarded for the comparison due to the low SNR and repeatability values, which results in errors during comparison. This is also shown in Fig. 10, where the accuracy given by the comparison with photogrammetry and repeatability (linked to the SNR) is presented. In fact, 7 of those 23 points given accuracies below 100 µm, which is in agreement to the conclusions drawn from the repeatability analysis carried out in AD.9 - Technical Note 5.1 (TN 5.1): "Facility Test Report". In conclusion, the metrology breadboard has shown the potential to characterize LDRs obtaining accuracies below 100 µm for the best points captured by the system. This means that being able to obtain SNR valuer similar to the best cases (40 dB) will result in a larger number of points (potentially 100) with accuracy below 100 µm. Already, some solutions to achieve this have been proposed to ESA.

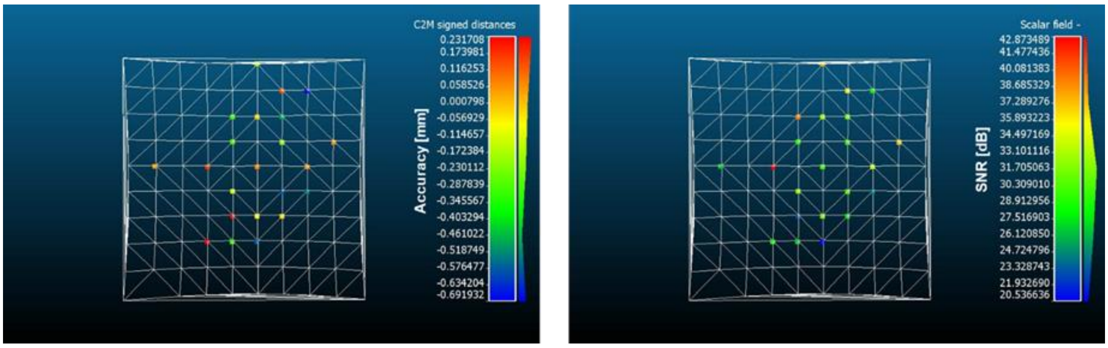


**Figure 9. Surface from the photogrammetry point cloud and selected best points (SNR and repeatability) from the metrology breadboard for the comparison.**

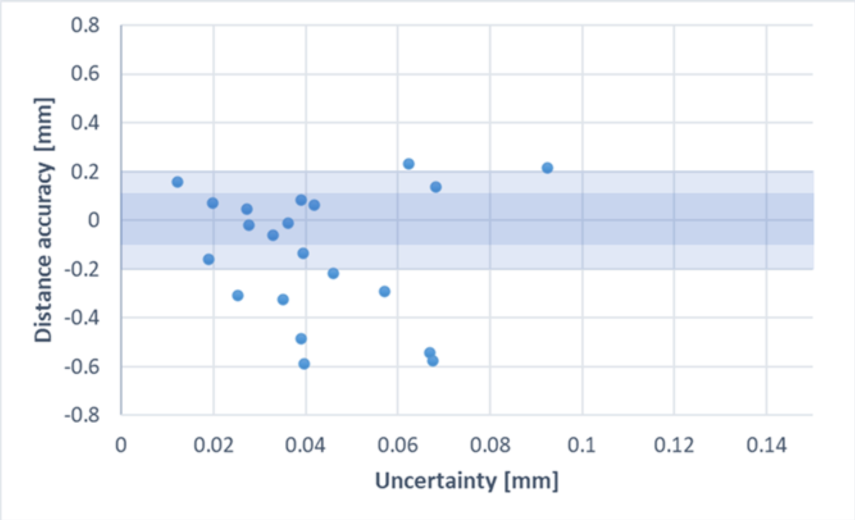


**Figure 10. Distance accuracy vs repeatability of the metrology system for the best points (SNR and repeatability) measured by the metrology breadboard.**

## 6. CONCLUSIONS

The metrology breadboard developed and manufactured has been tested on a 4.4 m diameter LDR built for the L-Band frequency range with an attainable accuracy of 10 µm for the locations of interest. The metrology instrument is completely akinetic and satisfies most of the requirements set at the beginning of the project based on real space missions, including compactness, limited power consumption and non-contact measurements at distance. Measurement time is reduced to less than few seconds compared to, for instance, days required by photogrammetry as seen during the test campaigns. Furthermore, the accuracy achieved brings the technology beyond what has been so far demonstrated with other technology offering also a path for in-orbit metrology of large structures.

## 7. CCN

During the CCN, improvements in hardware and software were implemented in the system in order to achieve the best performance of the system. Furthermore, absolute calibration of the breadboard was performed at the Spanish Metrology Center together with a second measurement campaign at Tekniker to measure the LDR mesh. Here, we concisely summarize all the findings given by the improved breadboard.

From the calibration at CEM (Fig. 1), we obtained a root mean square (RMS) error of 40 µm at 20 m for a single point. This means that the absolute accuracy or absolute deviation from the national distance standard of 40 µm, close to the target of 10 µm aimed at the beginning of the project.

**Figure 1. Breadboard setup for measurements at CEM**

Furthermore, a second measurement campaign at Tekniker (Fig. 2) was performed for a second comparison of point clouds (100 points) with the previous measurements given by photogrammetry. The resulting measurements regarding the uncertainty of the measurements and the point cloud are given in Fig. 3. Here we can see that the improvements of the breadboard led to obtain 100 points measured instead of 81 as during the main project. This is one of the main achievements as the full performance of the system is recovered. Furthermore, the SNR increase resulted in uncertainties (given by the standard error) below 80 µm for 69 out of the 100 points and 20 µm for 55 of those points, which is within the requirements for the system during the project.

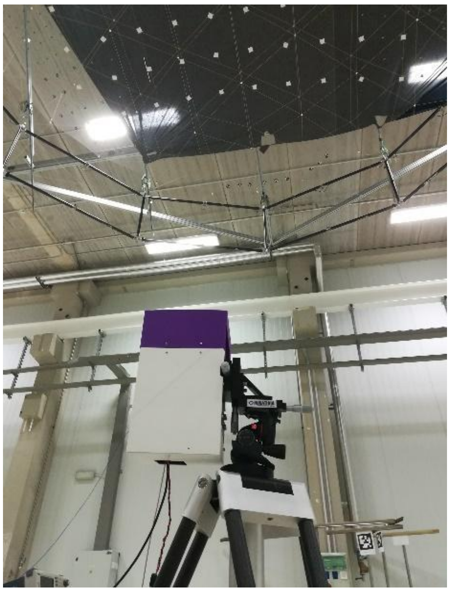

**Figure 2. Breadboard setup for the measurements of the LDR**

From the comparison with photogrammetry, it was concluded that the measurements with photogrammetry were not able to provide an absolute baseline measurement for the LDR, given the constraints of the setup. These constraints included measurements taken at different points within the marker as photogrammetry is restricted to the central points of the markers. A solution for this would be to perform the measurements at the same time, monitoring with an IR camera where the breadboard is pointing and then doing both measurements. This was not possible during the CCN because only measurements with the breadboard system were performed, so the comparison was done with a point cloud from the first campaign.

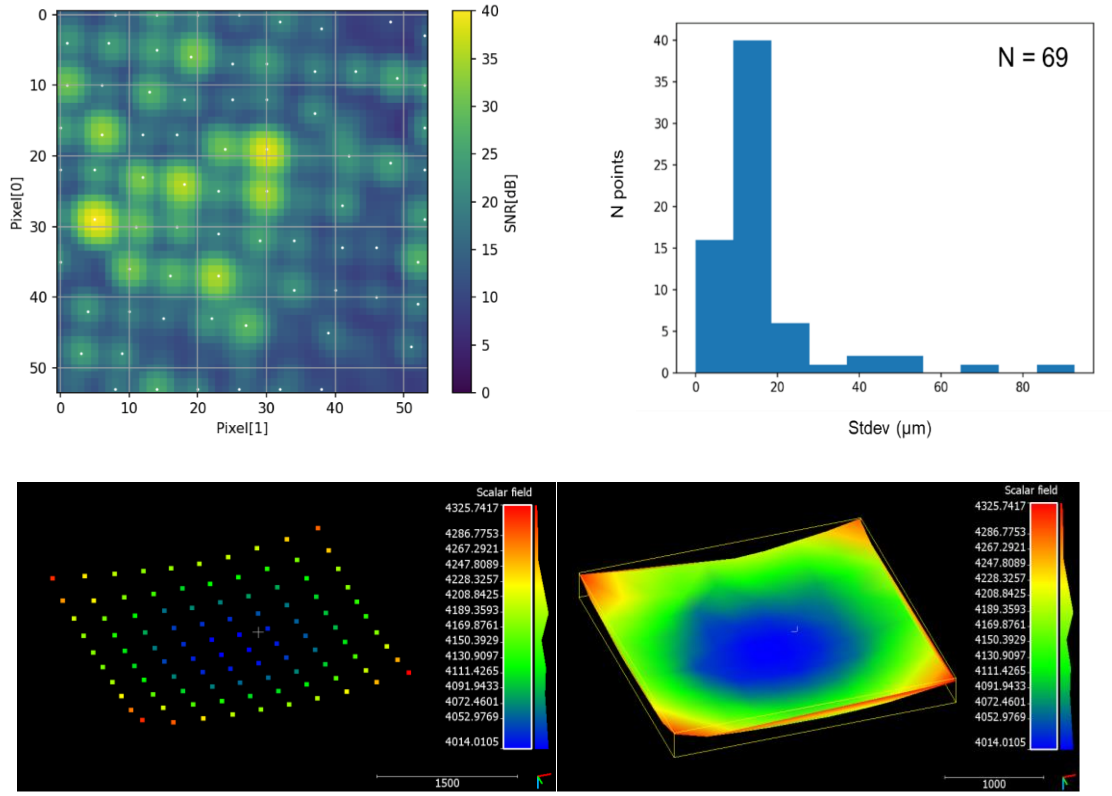


**Figure 3. Points measured by the breadboard (top-left) and standard error of each of them (top-right). Point cloud and reconstructed surface from the results given above.**

In conclusion, all the activities planned for the CCN were successfully performed. All hardware and software improvements resulted in a better performance of the breadboard system. This included full performance regarding the number of points measured (100 out of 100) and uncertainties below 80 μm for 70% of the 100 points measured on the LDR. Moreover, the breadboard system was calibrated for individual points at the Spanish Metrology Center, resulting in an accuracy of 40 μm at 20 m. On the hand, it was found that the comparison with photogrammetry on the 100 points was not possible due to constraints of the setup. In overall, the outcome from the CCN and the overall project is successful as a metrology system for space at TRL4 was developed, offering good performance.

## 8. References

1. Qi, X., Huang, H., Li, B., & Deng, Z. (2016). A large ring deployable mechanism for space satellite antenna. Aerospace Science and Technology, 58, 498-510.

2. Webb, D., Kasdin, N. J., Lisman, D., Shaklan, S., Thomson, M., Cady, E., ... & Lo, A. (2014, July). Successful Starshade petal deployment tolerance verification in support of NASA's technology development for exoplanet missions. In Advances in Optical and Mechanical Technologies for Telescopes and Instrumentation (Vol. 9151, p. 91511P). International Society for Optics and Photonics.

3. Schmitt, R. H., Peterek, M., Morse, E., Knapp, W., Galetto, M., Härtig, F., ... & Estler, W. T. (2016). Advances in large-scale metrology–review and future trends. CIRP Annals, 65(2), 643-665.

4. Bedukadze, G., & Datashvili, L. (2014). Some problems in ground testing of large space lightweight structures. In Proceedings of the 2nd International Conference on Advanced Lightweight Structures and Reflector Antennas, Tbilisi, Georgia.

5. Datashvili, L., Baier, H., Endler, S., Maghaldadze, N., Friemel, M., Luo, T., & Santiago-Prowald, J. (2014). Dimensional stability and shape-accuracy of shell-membrane reflecting surfaces made of fiber-reinforced elastomers. In International Conference on Advanced Lightweight Structures and Reflector Antennas.

6. Dumm, J. J., Boyle, M. P., & Clancy, J. P. (2013). High-Fidelity Antenna Pattern Modeling with Lidar Characterization. Johns Hopkins APL Technical Digest, 31(3), 263-275.